11-21

Identification of Subgrade Characteristics From Prototype Testing of Landing Mats

JOHN C. ROSNER, Department of Civil Engineering, Arizona State University; and MILTON E. HARR, Department of Civil Engineering, Purdue University

•SURFACE MATERIALS distribute wheel loads to the subgrade in a complicated manner, and the exact mechanism through which distribution is accomplished has not been defined. The consensus is, however, that the surface materials distribute loads in a manner similar to that of a beam or flat plate (1, 6, 10). Regardless of the load transfer mechanism chosen or the sophistication attached thereto, characterization of the subgrade is made presently from indicators (properties) obtained from selected samples imposed to artificial stress conditions. These indicators are then employed with design charts and/or formulas, which have been judiciously tempered by experience, to estimate the life of a pavement system.

Present design procedures have merit as long as the proposed traffic loading and subgrade conditions can be related adequately to past experience. However, application of these pavement design procedures to future traffic demands may prove unsatisfactory, and hence other design approaches should be sought to accommodate future needs. The hypothesis is forwarded in this paper that such developments are consequent upon the mechanistic modeling of pavements to reflect their behavior as demonstrated in prototype tests.

Mechanistic simulation of prototype tests provides a means whereby the system parameters can be determined from the pavement behavior under actual stress conditions. In addition, such an approach permits investigation of the pavement system at times other than failure.

DESCRIPTION OF PROTOTYPE TESTS

In 1966, accelerated traffic tests simulating aircraft taxiing operations were conducted by the Corps of Engineers (4) on test sections surfaced with landing mats. Numerous combinations of wheel configurations, loads, tire pressures, and subgrade strength were investigated. The wheel configuration varied from that of a single wheel up to a combination of 12 wheels; loadings varied from 35,000 to 273,000 lb; and tire pressures ranged from 50 to 250 psi. Two soils were used as subgrade materials. One soil was a "fat clay (CH)" with a liquid limit of 58 and a plasticity index of 31, while the other soil was a "fat clay (CH)" with a liquid limit of 61 and a plasticity index of 37. The in-place, initial strength of these subgrades as indicated by CBR values ranged from 1.1 to 9.0.

The tests were made on the modified T11 mat (designated herein as Item 1), which is a lightweight, extruded aluminum panel with an abrasive surface, and on the M8 mat (Item 2), which is a heavy deep-ribbed steel mat. The moment of inertia per foot of width of these two mats is 1.368 $in.^4$ and 0.618 $in.^4$ respectively. Both mats were placed on the subgrade in a masonry type of arrangement, as shown in Figure 1.

The behavioral characteristics and performance of the mat surfaces, whether loaded or unloaded, are well documented in the Corps of Engineers' publication (4) for each test at the various coverage levels. The data, single-wheel and dual-wheel, from this series constitute the basis of the investigation reported herein.

Paper sponsored by Committee on Theory of Pavement Design.

MECHANISTIC ANALYSIS

Model Development

A mechanistic model was sought whose deflection behavior reflected the action of observed landing mats. Initial consideration was given to the selection of a representative structural load transfer element. Following earlier findings of the Corps of Engineers (2), a membrane and thin plate were quickly eliminated as possibilities.

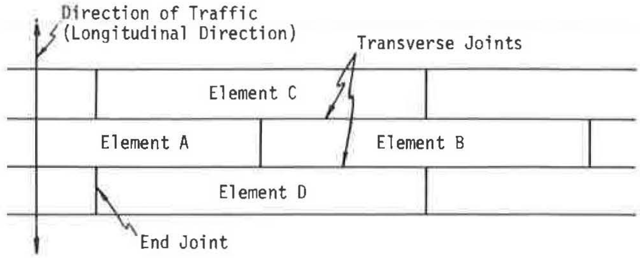

Figure 1. Arrangement of mat elements within the traffic lane.

A beam of infinite length was selected as the mechanistic equivalent of the mat. This selection was predicated on several prevailing conditions. First, actual field operations and test procedures employed by the Corps of Engineers (4) demonstrated that the mat elements extend laterally for an appreciable distance outside the normal traffic lane. Second, the transverse joints in the mat surface (necessitated by the construction procedure) provided virtually no moment transfer from one row of mats to the next (Fig. 1). Also, tests (2) on the M8 mat indicated that the transverse rigidity was approximately 150 times larger than the longitudinal rigidity.

A second approximation was necessary to "idealize" the soil media. Because prototype tests (4) indicated that the "average deflection" increased with the number of coverages, a conventional elastic solid model was not thought to be directly applicable. The observed behavioral characteristic was accommodated by employing a "quasi-elastic" model wherein parameters are permitted to be coverage-dependent.

The width of the infinite beam was taken as the length of a rectangle whose area was equivalent to the tire print area and whose width was equal to the maximum width of the tire print.

In addition, the following assumptions were made:

1. The end joint connections provide total shear and moment transfer between mat elements;
2. The wheel loads can be represented by uniformly distributed loads;
3. The beam obeys Eulerian conditions regardless of the stress level;
4. The beam and the soil always remain in contact; and
5. Horizontal displacements within the soil media are negligible.

The validity of the assumption of complete moment transfer was investigated by Rosner (8). Results indicated that the effectiveness of the end joint connections was approximately only 10 to 15 percent less than that of the mat elements.

Mat-soil parameters were established by analytical simulation of the prototype test data. This was achieved through a modification of the general variational method of analysis developed by Vlasov and Leont'ev (9).

Imposing the foregoing assumptions, the response of the mat-soil model was expressed as

$$\frac{d^4V(\eta)}{d\eta^4} - 2r^2\frac{d^2V(\eta)}{d\eta^2} + s^4V(\eta) = \frac{p(x)L^4}{EI} \tag{1}$$

where

$$r^2 = \frac{tL^2}{EI} = \frac{1 - \mu_0}{2L}\int_0^H \Psi^2 dy \tag{2}$$

$$s^4 = \frac{kL^4}{EI} = 2L \int_0^H \left[\frac{d\Psi(y)}{dy}\right]^2 dy \tag{3}$$

and

$$L = \sqrt[3]{\frac{2EI(1 - \mu_0^2)}{E_0\delta}} \tag{4}$$

and where

- E is the modulus of elasticity of the beam (mat),
- E_0 is the modulus of elasticity of the soil,
- H is the thickness of the soil layer,
- I is the moment of inertia of the beam,
- k is a foundation modulus that determines the compressive strains in the foundation,
- L is an elastic characteristic of the model,
- p(x) is a uniform loading function,
- t is a foundation modulus that determines the shearing strains in the foundation,
- $V(\eta)$ is the generalized deflection,
- δ is the width of the beam,
- μ_0 is Poisson's ratio of the soil, and
- $\Psi(y)$ is a function representing the distribution of displacement with depth (y).

It should be noted that Eq. 1 differs significantly from the governing relationship for an infinite beam on a Winkler foundation. The third term on the left-hand side of Eq. 1 arises from consideration of the normal strains within the soil; the coefficient on this term is analogous to the Winkler spring constant. The second term of Eq. 1 accounts for the presence of shearing strains within the soil; this term does not appear in the Winkler model. The coefficients for these two terms can be related to the distribution of displacement with depth as shown in Eqs. 2 and 3.

Tests conducted by the Corps of Engineers (2) indicated an asymptotic attenuation of displacements with depth. Functional representation of this type of displacements may take many forms. One convenient form, suggested by Vlasov and Leont'ev (9), assumes a ratio of hyperbolic functions as

$$\Psi(y) = \frac{\sinh \gamma\left(\frac{H - y}{L}\right)}{\sinh \frac{\gamma H}{L}} \tag{5}$$

where y is the distance from the subgrade surface and γ is a dimensionless parameter that reflects the rate of attenuation of displacement with depth.

With the distribution of displacements described by Eq. 5, the stresses can be expressed as

$$\sigma_y = \frac{E_0}{1 - \mu_0^2} V(x) \frac{d\Psi(y)}{dy} \tag{6}$$

and

$$\tau_{xy} = \frac{E_0}{2(1 + \mu_0)} \frac{dV}{dx}(x)\Psi(y) \tag{7}$$

A representation of the distribution of the above stresses on a vertical section through the soil mass is given in Figure 2.

With the form of $\Psi(y)$ taken as in Eq. 5, any variation in the rate of attenuation of the displacement can be incorporated by judicious selection of the parameter γ (Fig. 3). The value of γ could not be established directly from any previous studies. Hence, a simulation procedure was evolved that could yield reasonable measures of this parameter from the "average deflection" patterns.

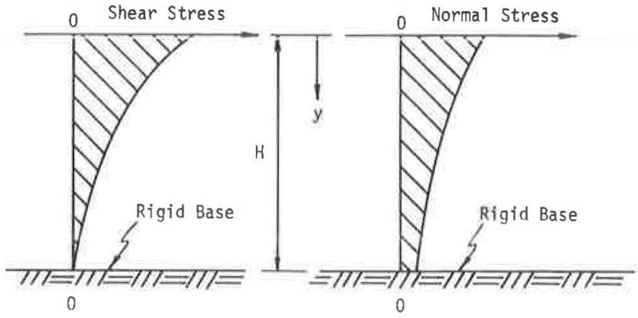

Figure 2. Distribution of stresses with depth.

For simplicity it was assumed that the soil media extended to infinite depth. Under this assumption, the model characteristics k and t in Eqs. 2 and 3 become

$$k = \frac{E_0\delta}{2(1 - \mu_0^2)} \frac{\gamma}{L} \tag{8}$$

$$t = \frac{E_0\delta}{8(1 + \mu_0)} \frac{L}{\gamma} \tag{9}$$

Parameter Indentification

The model characteristics k and t (Eqs. 8 and 9 are functions of γ in addition to the conventional elastic constants, E_0 and μ_0. Previous studies of beams on elastic foundations indicated that variation of μ_0 generally has a negligible effect on resulting deflection patterns. In this study μ_0 is assigned a value of 0.4 as had previously been suggested by Pickett (6, 7). Any error introduced by this assumption can be compensated for by the remaining parameters E_0 and γ as they are identified in the simulated procedure.

Loads were imposed on the developed mat-soil model similar to those of the prototype tests. The "steep descent" method (5) was employed for the identification of the model parameters. The criterion imposed was to minimize an error functional (the sum of the square of the differences between the actual deflection and the model deflection of at least 9 discrete points).

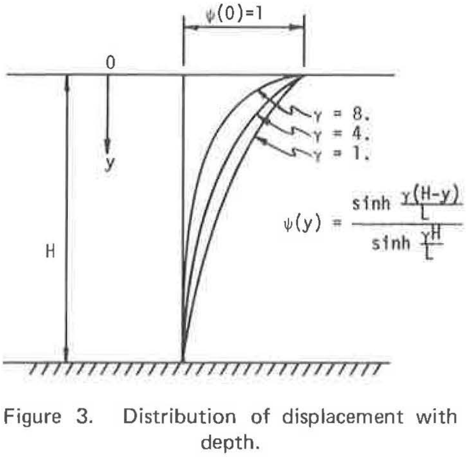

Figure 3. Distribution of displacement with depth.

The foregoing procedure was applied initially to data gathered from the Corps of Engineers' test designated as section 1, lane 2, item 1, for zero coverages. The initial values assumed for E_0 and γ were 100 psi and 1.55 respectively. A minimum of the error functional of 0.060 was achieved when E_0 = 750 psi and γ = 1.598; this is indicated as trial 1 in Figure 4. To determine whether the minimum obtained was global rather than local, another trial was performed. Trial 2 (Fig. 4), which was initiated with E_0 = 200 psi and γ = 6.00, produced a minimum of 0.079 when E_0 = 280 psi and γ = 6.006. From these results it was apparent that the surface of the error functional was definitely not bowl-like in form. Additional trials were made as indicated in Figure 4. As can be seen from the figure, the error functional possessed a curved

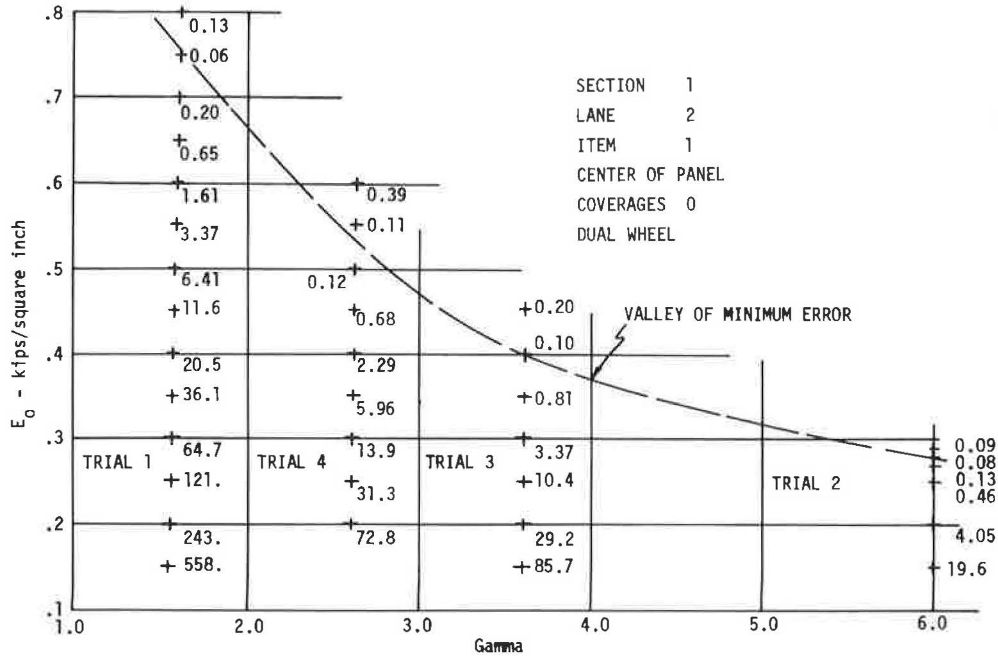

Figure 4. Behavior of error functional (section 1, lane 2, item 1).

valley of minimal values that for all practical purposes could be considered identical.

It was apparent that unique values of E_0 and γ could not be obtained with the selected form of the error functional. Fortunately, as can be seen in Table 1, the values of the parameter k varied only slightly along the valley of the error functional. This behavior was found to be general (8), and hence representative values of the characteristic k were generated.

Since the line of steepest descent for all trials (Fig. 4) was essentially parallel to the E_0 axis, a modification was incorporated into the identification procedure. Values of 1.0, 2.5, 4.0, 5.5, 7.0, and 8.5 were assigned to the parameter γ and for each of these values E_0 was incremented until the error functional was minimized. This procedure was subsequently employed for the determination of the parameter k for all relevant test sections and at all coverage levels.

Because of the insensitivity of the error functional to large change in γ, it was concluded that the developed procedure was not satisfactory. Preliminary studies (Fig. 5) indicated that the magnitude of the computed deflections was not sensitive to changes in γ. However, as γ increased, deflections in the near vicinity of the loads did become larger and attenuated more rapidly with lateral distance than the observed pattern. This seemed to indicate that the value of γ was related to the rigidity of the mat; that is, the more flexible the mat, the larger the deflection under the load and the more rapid the return to the undeflected position.

The parameter γ was established by a trial-and-error procedure using generated computer model deflections. The value of k (previously and independently determined) was held constant for each coverage level while different values were assigned to γ. The "correct" value of γ was established

TABLE 1

VALUES OF k ALONG THE VALLEY OF THE ERROR FUNCTIONAL

Section 1 E_0	Lane 2 γ	Item 1 Error	Zero Coverage k
750 psi	1.598	0.060	52.5 pci
530 psi	2.620	0.095	52.4 pci
400 psi	3.608	0.100	51.0 pci
280 psi	6.006	0.079	52.8 pci

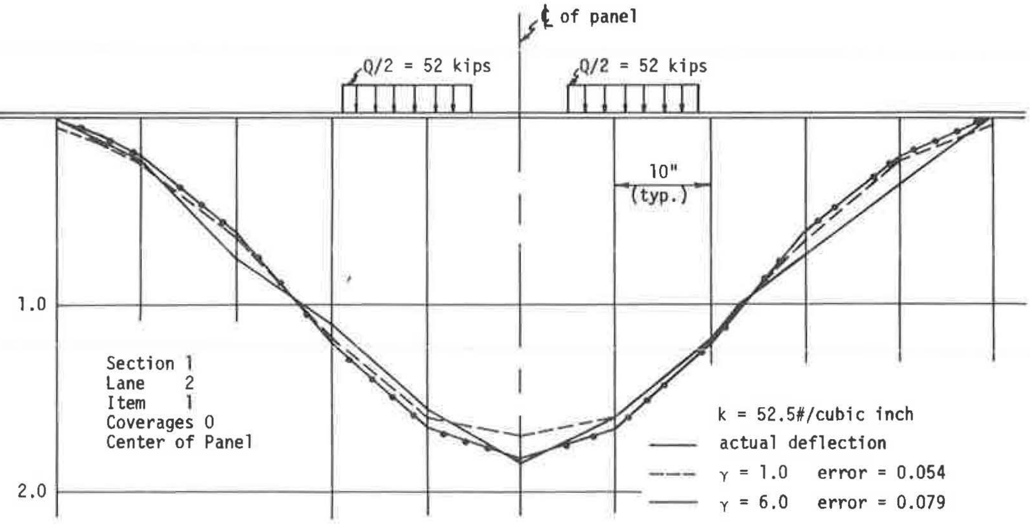

Figure 5. Influence of the parameter γ on the deflection pattern.

by comparing the computed model deflection configuration to the prototype deflection pattern. After the parameter γ had been established, slight modifications were made in the initial value of the parameter k to improve the correspondence between deflection patterns. This procedure was followed in all subsequent cases to obtain measures of both γ and k values.

RESULTS

Values of the parameters γ, E_0, k, and the error functional for two typical test sections are given in Table 2. Displaying the magnitude of k against the number of coverages (Fig. 6) it can be observed that, in general, the magnitude of the parameter k decreases with coverage. Similar behavior was also observed for the dual-wheel tests (8).

It was found that the magnitude of k at any coverage level could be established as a function of the initial value. This relationship was established empirically as

$$k_N = \frac{k_{INT}}{N^{0.0485}} \qquad (10)$$

where k_{INT} is the k value at zero coverage and k_N is the k value after N number of coverages. The value of k_{INT} was found to correlate with several standard soil properties: water content, dry density, and CBR (obtained at the test site). It was found for the prototype tests that k_{INT} could be established from the relationship

$$k_{INT} = 164.0 + 3.0\ \mathrm{CBR} - 5.4w\ \gamma_d \qquad (11)$$

where CBR is the average CBR for the upper 18 in. of subgrade and w γ_d is in pounds per cubic foot.

Observations of the "average deflection" patterns of the prototype tests indicate that the curvature, in general, increased with increasing number of coverages. The identification procedure demonstrated that the value of γ also increased with coverages and

TABLE 2

COMPARISON OF THE VARIABILITY OF THE CHARACTERISTIC k

γ	E_o, psi	k, pci	Error	E_o, psi	k, pci	Error
		Section 2 Lane 3 Item 1				
	Coverage zero				Coverage 600	
1.0	800	36	0.139	680	29	0.040
2.5	420	38	0.108	350	30	0.043
4.0	290	37	0.105	250	30	0.043
5.5	230	37	0.103	200	31	0.044
7.0	190	37	0.104	170	32	0.050
8.5	170	38	0.102	150	32	0.061
		Section 9 Lane 21 Item 2				
	Coverage zero				Coverage 20	
1.0	540	25	0.080	510	24	0.064
2.5	280	26	0.058	270	25	0.045
4.0	200	27	0.055	190	25	0.043
5.5	160	27	0.054	160	28	0.051
7.0	140	29	0.058	130	27	0.041
8.5	120	29	0.053	110	26	0.052
		Section 9 Lane 21 Item 2				
	Coverage 200				Coverage 300	
1.0	480	22	0.626	460	21	0.166
2.5	250	23	0.528	240	22	0.128
4.0	180	24	0.510	170	22	0.126
5.5	160	28	0.597	160	28	0.365
7.0	120	24	0.509	120	24	0.127
8.5	110	26	0.500	110	26	0.182

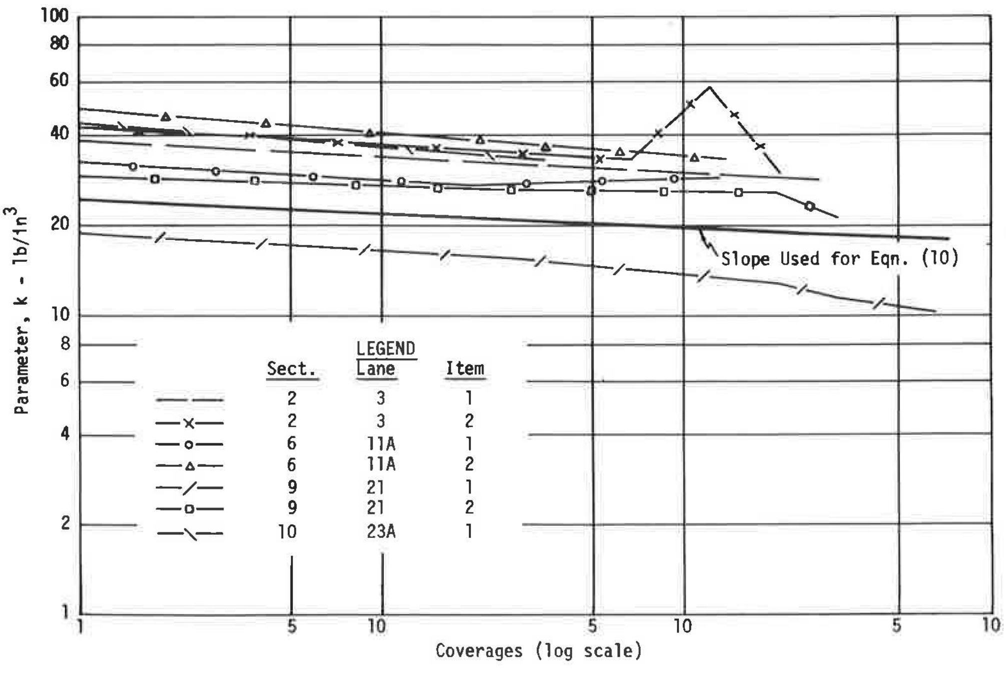

Figure 6. Variation of parameter k with coverage for single-wheel tests.

TABLE 3

COMPARISON OF DEFLECTION PATTERNS

Distance (in.)	Actual Deflection (in.)	Estimated Deflection (in.)	Distance (in.)	Actual Deflection (in.)	Estimated Deflection (in.)
Section 2 Lane 3 Item 1					
k_{INT} = 35.5 pci γ_{INT} = 1.00					
Zero Coverages - Error = 0.139			600 Coverages - Error = 0.164		
99	0.10	0.20	90	0.00	0.09
102	0.15	0.26	102	0.42	0.38
105	0.19	0.33	112	0.71	0.76
112	0.41	0.54	120	1.00	1.11
117	0.59	0.71	132	1.19	1.41
122	0.88	0.87	142	0.96	1.19
129	1.20	1.03	146	0.88	1.03
132	1.17	1.04	152	0.71	0.77
142	0.82	0.87	162	0.38	0.38
152	0.61	0.54	174	0.00	0.09
162	0.27	0.26			
170	0.00	0.11			
Section 9 Lane 21 Item 2					
k_{INT} = 25.5 pci γ_{INT} = 1.75					
Zero Coverages - Error = 0.063			300 Coverages - Error = 0.149		
108	0.00	0.12	108	0.00	0.18
114	0.20	0.24	114	0.28	0.36
124	0.55	0.56	120	0.57	0.58
134	0.90	0.93	124	0.59	0.75
144	1.15	1.11	132	1.00	1.12
154	1.00	0.93	134	1.15	1.20
164	0.70	0.56	144	1.32	1.41
174	0.20	0.24	154	1.27	1.20
179	0.00	0.14	160	1.00	0.94
			164	0.80	0.76
			174	0.32	0.36
			179	0.00	0.21

TABLE 4

COMPARISON OF SIMULATED TO CALCULATED VALUES OF k_{INT}

Section	Test Lane	Item	k, pci		Section	Test Lane	Item	k, pci	
			Simulated	Calculated				Calculated	Calculated
1	1	1	48.5	59.3	6	12	2	36.0	36.7
1	2	1	50.5	66.1	9	21	1	14.0	11.9
2	3	1	35.5	18.5	9	21	2	25.5	20.2
2	3	2	41.0	35.1	9	22	1	10.0	11.2
2	4	1	19.0	15.9	9	22	2	16.0	13.5
2	4	2	31.5	38.3	10	23A	1	37.5	27.1
3	5	1	16.0	17.0	10	23A	2	27.5	31.7
3	5	2	21.0	32.7	10	23B	1	32.5	27.1
3	6	1	12.5	20.4	13	28	1	11.0	11.6
3	6	2	18.0	29.2	13	28	2	25.0	25.3
6	11	1	34.0	20.6	13	29	1	18.0	11.7
6	11	2	50.5	41.8	13	29	2	28.0	24.2
6	12	1	22.0	29.4					

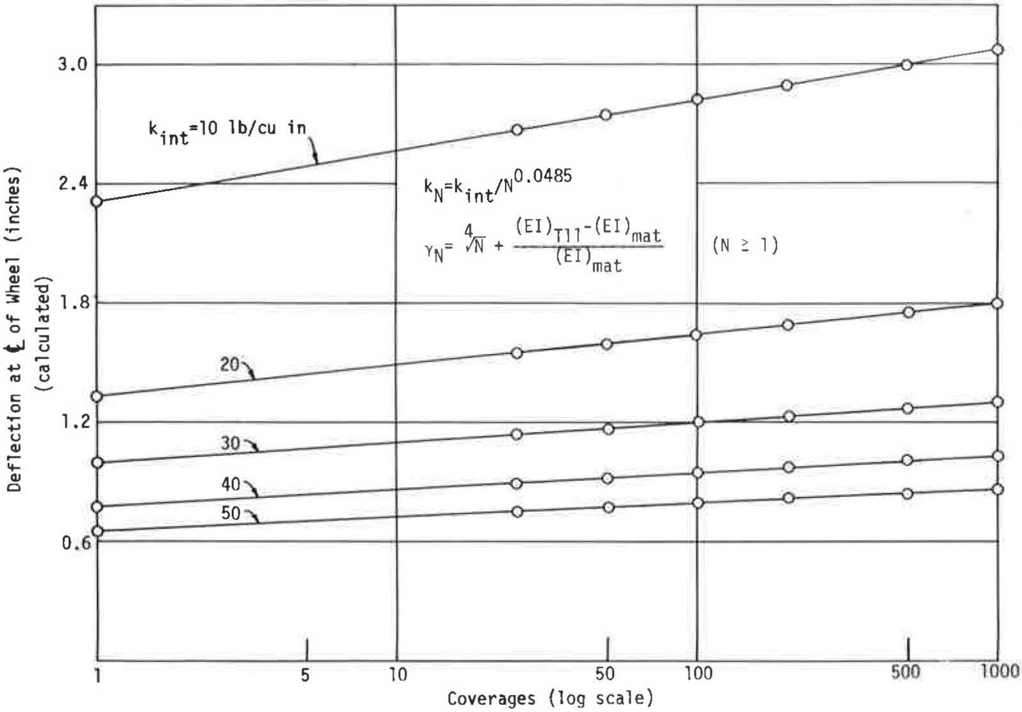

Figure 7. Influence of k_{INT} on maximum deflection.

became slightly larger with decreasing mat rigidity. The relationship for γ_N was established as

$$\gamma_N = \sqrt[4]{N} + \frac{(EI)_{T11} - (EI)_{MAT}}{(EI)_{MAT}} \quad (N \geq 1) \tag{12}$$

where N is the specific number of coverages, $(EI)_{T11}$ is the rigidity per foot of width of the T11 aluminum mat, and $(EI)_{MAT}$ is the rigidity per foot of width of the mat being investigated.

With the parameters k_{INT} and γ_N defined, the system characteristic t may be found from Eqs. 8 and 9. Some typical computed deflection patterns obtained using Eqs. 10 and 12 are given in Table 3. Some observed deflection patterns are also given.

In Table 4 are given values of k_{INT} obtained from the identification procedure and from Eq. 11. It is noted that the largest discrepancies occur for those sections where the simulated values were high. From Figure 7, it can be observed that small variations in the subgrade strength, as reflected by the subgrade modulus, have appreciable influence on the deflection characteristics of the load transfer element.

SUMMARY AND DISCUSSION

The model characteristics k and t (Eqs. 8 and 9), are functions of γ in addition to the conventional E_0 and μ_0 parameters. The "steep descent" method used for identification failed to produce unique values of the parameters E_0 and γ (Fig. 4). However, the error functional was found to possess a valley of minimums along which the value of the characteristic k was found to be essentially constant.

The simulation of the "average deflection" patterns (Table 2) indicated that the value of the model parameter k increased slightly with increases in γ. For a specific value of γ (as shown in Table 2) the magnitude of k was found to decrease with the number of coverages. Computations indicated that the magnitude of k was more sensitive to the number of coverages than to the value of the parameter γ. The validity of the developed expression for k_N (Eq. 10) is demonstrated in Table 2 and Figure 6.

As noted in Figure 5, variations in the parameter γ were reflected primarily as alterations of the deflection pattern curvature. The representative value of γ was established from the similarity of model deflection curvature for various values of γ with prototype deflection curvature. From this comparison it was noted that the curvature, and thus γ, increased with coverages and decreased with increasing mat rigidity. This behavior is expressed by Eq. 12.

The simulated values of the characteristic k at zero coverages were in all cases less than 53 pci. In this range, the model deflections were found to be quite sensitive to the magnitude of k_{INT} (Fig. 7).

CONCLUSIONS

On the basis of assumptions made herein, the following conclusions appear warranted:

1. A mechanistic model can be developed that is capable of duplicating the behavior of prototype landing mat systems under static loads.
2. Numerical values for parameters entering the model can be obtained from simulation of prototype deflection patterns.
3. Model parameters can be correlated with established soil properties.
4. Contrary to prevailing opinion, the subgrade modulus (k) decreased as trafficking progressed and the associated model behavior is extremely sensitive to the magnitude of the subgrade modulus.

ACKNOWLEDGMENT

This work was performed at Purdue University as part of a project sponsored by the Flexible Pavement Branch, Soil Division, Corps of Engineers, U.S. Army Waterways Experiment Station, Vicksburg, Mississippi. The assistance of Messrs. Richard G. Ahlvin and Thomas White of that Branch is greatly acknowledged.

REFERENCES

1. Burmister, D. M. Theory of Stresses and Displacements in Layered Systems and Applications to the Design of Airport Runways. HRB Proc., Vol. 23, 1943, pp. 126-144.
2. U.S. Army Corps of Engineers. Theoretical Landing Mat Studies. Tech. Memorandum No. 3-418, Waterways Experiment Station, Vicksburg, Miss., Oct. 1955.
3. U.S. Army Corps of Engineers. Engineering Tests of Experimental T11 Aluminum Airplane Landing Mat. Tech. Report No. 3-634, Waterways Experiment Station, Vicksburg, Miss., Sept. 1963.
4. U.S. Army Corps of Engineers. Aircraft Ground-Floatation Investigation. Tech. Documentary Report AFFDL-TDR-66-43, Parts I, II, III, IV, V, VII, X, XI, and XIII. Air Force Flight Dynamics Laboratory, Wright-Patterson Air Force Base, Ohio, 1966.
5. Noble, B. The Exploration of Functional Relationships—An Aspect of Optimization. Applications of Undergraduate Mathematics in Engineering. Macmillan, New York, 1967.
6. Pickett, G., et al. Deflections, Moments, and Reactive Pressures for Concrete Pavements. Kansas State College Bulletin No. 65, Oct. 1951.
7. Pickett, G. Analytical Studies of Landing Mats for Forward Airfields. Final Report to Corps of Engineers, Waterways Experiment Station, Vicksburg, Miss., Dec. 1951.
8. Rosner, J. C. Theoretical Study of Landing Mat Behavior. Doctoral thesis, Purdue Univ., Aug. 1969.

9. Vlasov, V. Z., and Leont'ev, N. N. Beams, Plates, and Shells on an Elastic Foundation (translated from Russian). Israel Program for Scientific Translations, Jerusalem, 1966.

10. Westergaard, H. M. Stresses in Concrete Pavements Computed by Theoretical Analysis. Public Roads, Vol. 7, No. 2, 1926, pp. 25-35.